Available online at www.sciencedirect.com
SCIENCE DIRECT®
Journal of Power Sources 128 (2004) 247–255
JOURNAL OF POWER SOURCES
www.elsevier.com/locate/jpowsour

Transport properties of hectorite based nanocomposite single ion conductors

Ruchi Gupta Singhal [a], Michael D. Capracotta [b], James D. Martin [b], Saad A. Khan [a], Peter S. Fedkiw [a,*]

[a] *Department of Chemical Engineering, North Carolina State University, Raleigh, NC 27695-7905, USA*
[b] *Department of Chemistry, North Carolina State University, Raleigh, NC 27695-7905, USA*

Received 5 September 2003; accepted 29 September 2003

Abstract

The ionic conductivity and rheological properties of clay filled nanocomposite electrolytes are reported. These electrolytes, which have potential use in lithium-ion batteries, consist of lithium-exchanged hectorite, a 2:1 layered smectite clay, dispersed in ethylene carbonate (EC) or a mixture of EC + polyethylene glycol di-methyl ether (PEG-dm, 250 MW). All samples exhibit elastic, gel-like characteristics and room temperature conductivities of order 0.1 mS/cm. A maximum in conductivity is observed at about 25 wt.% clay concentration. A maximum in hectorite basal layer spacing is also observed in the same concentration range, suggesting a direct correlation between conductivity and layer spacing. The elastic modulus and yield stress increase by two orders of magnitude and the conductivity increases by one order of magnitude with increase in hectorite concentration from 5 to 25%, which indicates the significant influence of hectorite content in determining the characteristics of these single-ion conductors. The solvent composition plays a secondary role in this regard, with addition of PEG-dm to the base EC + hectorite electrolyte producing moderate improvement in conductivity. Similarly, the addition of PEG-dm to EC + hectorite affects an increase by only a factor of three in the elastic modulus and yield stress of the electrolyte.

Keywords: Lithium-ion cell; Composite gel electrolyte; Clay nanocomposite; Hectorite; Polyethylene glycol; Small angle X-ray diffraction

1. Introduction

Rechargeable lithium-ion batteries are an important component in portable electronic devices because of desirable characteristics that include high energy density, low weight, and excellent cycle performance. For instance, in 1997 alone, worldwide sales of rechargeable lithium-ion batteries exceeded 1.6 billion dollars [1]. Because of government mandates for electric vehicles and the ever-increasing demand for portable power sources, rechargeable lithium batteries are expected to grow more than 20% per year [2,3]. Lithium-ion batteries in particular are predicted to last the lifetime of a car because of their high energy and power density [4,5]. However, several factors in lithium-ion batteries, especially in the electrolyte, have limited commercial usage. Most lithium-ion batteries use a liquid electrolyte, which requires the use of a microporous polymeric membrane to separate the electrodes. As an alternative, our group [6] is attempting to avoid a separator by using a gel electrolyte with high-mechanical strength. These gel electrolytes must possess comparable electrochemical properties to liquid electrolytes such as conductivity, lithium transference number, and electrode/electrolyte interfacial stability. The technological impact of developing an electrolyte with improved conductivity and strong mechanical strength is significant and warrants further exploration.

Composite polymer electrolytes (CPE) are viable candidates for rechargeable batteries because they possess desirable properties of both liquid and solid electrolytes. Nano-size fillers such as TiO_2, SiO_2, or Al_2O_3 have shown many advantageous effects on electrochemical properties, (e.g., conductivity and transference number) of CPE [7–9]. The benefit of some fillers when added to a liquid solvent is their ability to create a gel-like matrix making a low-resistance, open-channel structure for ion transport. However, most fillers are passive, and function only as a structural skeleton. We, on the other hand, focus on an active filler, lithium hectorite, which provides both the ion-transport capability and mechanical strength.

Hectorite and other 2:1 layered clays (smectites) are characterized by a large negatively charged plate-like structure

* Corresponding author. Tel.: +1-919-515-3572; fax: +1-919-515-3465.
E-mail address: fedkiw@eos.ncsu.edu (P.S. Fedkiw).

0378-7753/$ – see front matter © 2003 Elsevier B.V. All rights reserved.
doi:10.1016/j.jpowsour.2003.09.064

(∼250 nm diameter) with exchangeable counter cations sandwiched between thin platelets (∼1 nm). For lithium battery application, the native sodium cations on hectorite are exchanged for lithium cations and the plate-like particles are dispersed in high-dielectric solvents (e.g., ethylene carbonate (EC) and propylene carbonate (PC)) to create a physically gelled structure. The cation mobility is considerable relative to the mobility of the large anion clay platelets.

Lithium-ion transference numbers in carbonate solvents with hectorite were shown to be near unity, which indicates predominantly lithium-ion mobility [10]. Conductivity at room temperature, however, in these electrolytes is around 10^{-4} S/cm, whereas that in a typical Li-ion battery electrolyte ($LiPF_6$ + EC + PC) is around 10^{-2} S/cm. High-molecular weight polyethylene oxide (PEO) has been shown to increase basal spacing of clay platelets [11], however, the ionic conductivity (10^{-6} S/cm) is four orders of magnitude below non-polymer electrolytes. Motivated by an anticipated increase in basal spacing induced by more mobile, low-molecular weight PEO, we have investigated the combined influence of low-molecular weight methyl terminated PEO, polyethylene glycol di-methyl ether (PEG-dm), with a carbonate co-solvent and Li hectorite.

We report our investigation of the effect of PEG-dm on conductivity, basal spacing of platelets, and rheological properties in hectorite/carbonate electrolytes. Conductivity is measured using impedance spectroscopy to quantify ion motion. The microscopic structure of hectorite clay platelets is analyzed using low angle X-ray diffraction (XRD) to find platelet spacing after dispersion into solution. Rheological properties are investigated to find the gel modulus and yield stress of the electrolyte. Several combinations of clay and polymer loading are studied in an attempt to find an electrolyte with the highest conductivity. A preliminary comparison of rheological properties between hydroxyl terminated PEO (PEG) and PEG-dm as a polymer co-solvent with EC is also made.

2. Experimental

2.1. Electrolyte preparation

Sodium hectorite, provided by Hoechst (SKS-21, 88 meq./100 g), was mixed with LiCl to exchange sodium with lithium. The lithium counterion of the platelet was the only source of lithium in the electrolyte; no additional salt was added. De-ionized (DI) water (850 ml) and Na-hectorite (20 g) were blended with 150 ml of 0.75 M LiCl solution. The mixture was allowed to equilibrate for 1 day and then centrifuged. The supernatant was discarded and the process was repeated twice. After the final LiCl exchange, the clay solids were mixed with 1000 ml of DI water and centrifuged. The DI water rinse process was repeated two more times. The hectorite mixture was then placed in a 100 °C oven for a minimum of 3 days during which the gel solidified. The clay was subsequently rinsed with 100 ml methanol (denatured, Aldrich) in a glass frit filter three times to remove residual salts (LiCl and NaCl). Finally, the hectorite was dried at 70 °C and atmospheric pressure for at least 1 day to remove methanol. Elemental analysis of Li hectorite, ($Mg_{5.3}Li_{0.7}Si_8O_{20}(OH,F)_4Li_{0.7}$), was performed by Quantitative Technologies Inc. (Whitehouse, New Jersey) and is summarized in Table 1. Aluminum was found in the sample, which was not expected in the Hoechst SKS-21 hectorite, but is present in saponite, another smectite clay made by Hoechst. Discrepancy in values could occur because of incomplete cation exchange, impurities (saponite and other compounds), and elemental analysis error.

Table 1
Composition analysis of Li hectorite compared to expected weight percent based on formula of Li-hectorite SKS-21 ($Mg_{5.3}Li_{0.7}Si_8O_{20}(OH,F)_4Li_{0.7}$)

Elements	Expected weight (%)	Found weight (%)
Si	29.6	24.5
Mg	17.0	17.6
Li	1.3	0.99
Na	0	0.16
C	0	0.16
Al	0	0.07

A matrix of samples was investigated to understand the effect of polymer addition in the Li hectorite/carbonate mixture. In this study, the amounts of hectorite and polymer were adjusted. The ethylene carbonate solvent (EC, Aldrich) and the polymer co-solvents (PEG-dm 250 MW and PEG 200 MW, Aldrich) were made at three volume ratios 1:1 EC:PEG-dm, 2:1 EC:PEG-dm, and 1:1 EC:PEG. Control samples were also made where no polymer was added to the EC. Polymer-only control samples (both PEG-dm and PEG) were not studied because hectorite did not disperse in these neat solvents. Hectorite loading was determined as a percentage of solvent weight. Conductivity data are presented with hectorite concentration reported as either hectorite wt.% or mol hectorite/kg solvent. The Li hectorite loadings investigated were 5, 10, 15, 20, 25, 30, and 40% hectorite (0.044–0.352 mol hectorite/kg solvent). The solvents, EC (at 70 °C) and PEG-dm (at room temperature), were pre-mixed to the desired volumetric ratio (1:1 and 2:1). Anhydrous ethanol (Aldrich) was added to separate clay platelets, which assisted solvent intercalation. Since the order of addition of the components had an effect on the quality of the hectorite dispersion, the following sequence was kept consistent: (1) Li hectorite, (2) EC/PEG-dm mixture, (3) ethanol.

The technique for dispersing clay platelets in the solvents was critical to ion mobility. Ethanol was used, instead of water, to exfoliate the clay platelets in order to reduce additional water removal steps. Li hectorite + 15 ml EC/PEG-dm solvent + ∼40 ml ethanol were mixed at 6100 rpm using a Silverson L4RT high-shear laboratory mixer with a 3/8 in. mixing head. The mixture was brought to 70 °C while mixing on a heating plate in order to accelerate ethanol removal. When the volume of the sample was reduced to

approximately 20 ml from its initial volume of approximately 60 ml, the heat was turned off but mixing continued. Sets of samples were dried simultaneously for 30–60 min increments in a vacuum oven at 100 °C under ∼1 kPa. The sample was then transferred to a high-purity argon (99.998%) atmosphere glove box. The weight of EC that was evaporated in the vacuum oven was calculated by determining the weight difference before and after drying, and was typically ∼30% of the initial EC amount. This amount of EC was then added back to the sample through hand mixing until the added EC was uniformly distributed. Water content of the electrolytes was measured using a Mitsubishi Karl-Fisher CA-06 titrator with vaporizer VA-06. Small amounts of each sample (∼0.04–0.1 g) were taken from the glove box in sealed glass vials and tested for water content. Samples with water content between 200 to 300 ppm were considered satisfactory, while samples with water content higher than 300 ppm were dried again in a vacuum oven. Additional drying steps were performed until the moisture level was in the appropriate range.

2.2. Conductivity

Conductivity measurements were made using a PAR 273 potentiostat and 5210 lock-in amplifier (Princeton Applied Research) or a BAS-Zahner IM6e Impedance Analyzer (Bioanalytical Systems, Inc.). A cell consisting of two platinum electrodes in a capped glass vial was used [10]. A cell constant was determined for each cell using a standard KCl solution. Samples were added to these cells in the glove box to ensure low-moisture content. Conductivity was measured between 25 and 100 °C and the average of two runs is reported.

2.3. X-ray diffraction (XRD)

Basal spacing was determined using an Inel XRG 3000 X-ray diffractometer that employed Cu Kα radiation ($\lambda = 1.5405$ Å). The measurements were performed at 35 kV and 30 mA. All samples were loaded into 0.7 mm quartz capillaries and affixed to a rotating goniometer head. Data were collected in transmission geometry over $1.5^\circ < 2\theta < 120^\circ$ using a CPS-120 detector with a collection time of 4 h. The non-uniform surface of gel samples when placed on a flat plate sample holder makes collecting grazing angle (small angle) diffraction difficult. The use of a rotating capillary sample holder, however, alleviates this problem. Data were calibrated with respect to an external silicon standard.

2.4. Rheology

Dynamic rheological measurements were conducted on a rheometrics dynamic stress rheometer (DSR II) using a 25 mm parallel plate geometry for concentrations less than 20% clay. At higher concentrations of clay, a TA instrument stress rheometer (AR2000) with a 20 mm parallel plate geometry [12] was used because of instrumental limitations of the DSR II. A sinusoidally varying stress was applied to the sample, and the resulting elastic (G') and viscous (G'') moduli were obtained as either a function of frequency, or stress amplitude at a fixed frequency of 1 rad/s. Frequency spectra of G' and G'' were obtained at a stress/strain amplitude in the linear viscoelastic regime. The yield stress was found by applying increasing stress until the elastic modulus decreased precipitously. Creep measurements were recorded to obtain the steady state creep compliance J_e^o and the recoverable creep compliance $J_r(t)$. During a creep measurement, a stress ($\tau_0 = 200$ Pa) was applied for a specified time ($t = 600$ s), and strain was recorded. The stress was then removed and the recoverable strain was recorded for 3200 s. Steady state creep compliance J_e^o was found from the extrapolated point at $t = 0$ of the linear slope of compliance as a function of time in the initial applied stress regime (the linear slope represents the steady state deformation of sample from the initial stress). Recoverable creep compliance, $J_r(t) = \gamma_r(t)/\tau_0$, was calculated from the recovery strain (γ_r) and the applied stress, represents the recoil of sample after the stress is removed.

3. Results

3.1. Conductivity measurements

Fig. 1 displays the effect of temperature on conductivity for electrolytes containing 5, 25, and 40% clay. Within experimental uncertainty, most samples exhibit Arrhenius behavior, as indicated by the linear relationship between conductivity and $1/T$, but one sample (2:1 EC:PEG-dm) produced slight non-Arrhenius behavior. Conductivity at 25 °C as a function of clay concentration is shown in Fig. 2 for electrolytes with various solvents: 1:1 EC:PEG-dm, 2:1 EC:PEG-dm, and 1:1 EC:PC. The conductivity with 1:1 EC:PC solvent was measured by Riley et al. [10] and was mixed slightly different from the procedure used in this study (water instead of ethanol was used in the initial dispersion and a high-shear mixer was not used). We see a slight improvement in conductivity for the 2:1 EC/PEG-dm electrolyte when compared to the 1:1 EC:PC and 1:1 EC:PEG-dm solvent. At concentrations above 25% clay, 2:1 EC:PEG-dm and EC solvents displayed a decrease in conductivity. A maximum in conductivity with concentration of Li hectorite at 60 °C is also seen in Fig. 3 where EC:PEG-dm solvent mixtures are compared to the EC only control samples. At 60 °C the maximum conductivity for both 2:1 EC:PEG-dm and EC electrolytes occurs at 0.22 mol Li hectorite/kg solvent and is 0.60 and 0.49 mS/cm, respectively. The maximum conductivity for 1:1 EC:PEG-dm at 60 °C is 0.54 mS/cm and occurs at 0.26 mol Li hectorite/kg solvent. The result in Figs. 2 and 3 indicate that the concentration at which maximum conductivity occurs is approximately independent of temperature over this narrow

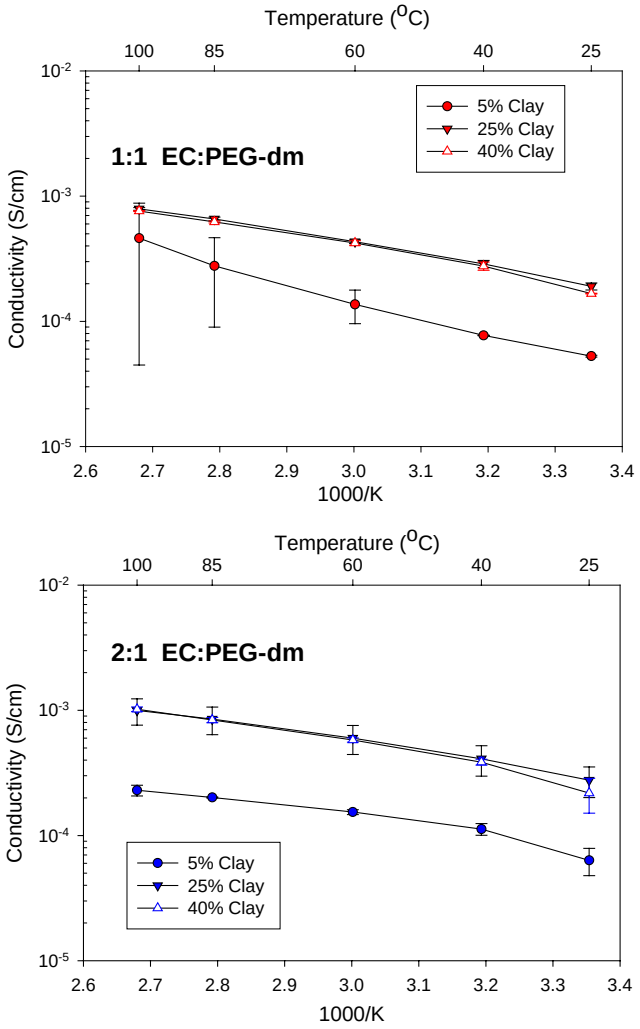

Fig. 1. Arrhenius plot of conductivity for 5, 25, and 40% Li-hectorite in 1:1 EC:PEG-dm (top) and 2:1 EC:PEG-dm (bottom) solvent mixture.

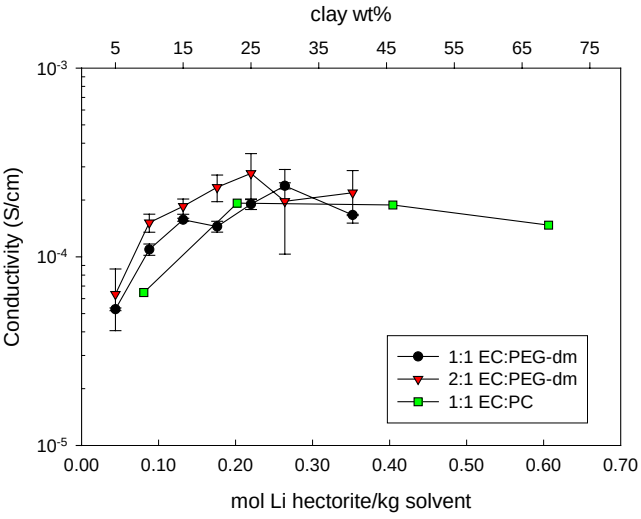

Fig. 2. Conductivity at 25 °C of clay-containing electrolyte for three solvent systems: 1:1 EC:PEG-dm, 2:1 EC:PEG-dm, and 1:1 EC:PC (Riley et al. [10]).

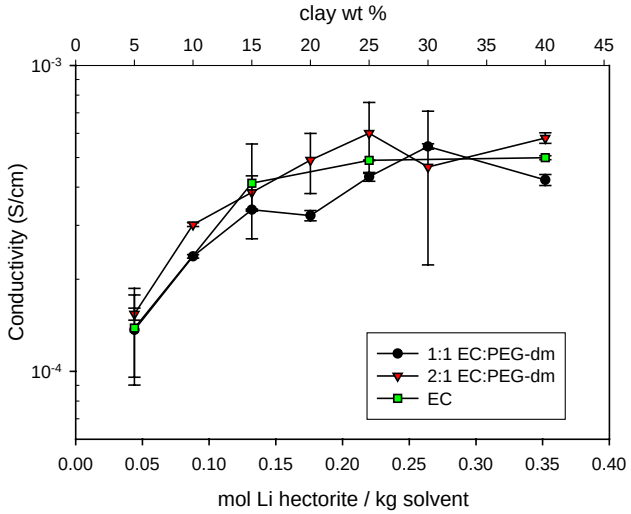

Fig. 3. Conductivity at 60 °C for of clay containing electrolyte for three solvent systems 1:1 EC:PEG-dm, 2:1 EC:PEG-dm, and EC only.

temperature range (25–60 °C). However, the maximum conductivity of 2:1 EC:PEG-dm electrolytes is 10% higher than the maximum conductivity of 1:1 EC:PEG-dm electrolytes at 25 °C and is 14% higher at 60 °C.

3.2. XRD measurements

Interlayer separation of clay platelets was determined using X-ray diffraction. Three solvents were investigated: 1:1 EC:PEG-dm, 2:1 EC:PEG-dm, and EC only, at four loadings of clay (5, 15, 25, 40 wt.%). The diffraction patterns are shown in Fig. 4. Two peaks are seen for powder Li hectorite, $2\theta = 2.3°$ and 6.9°, which corresponds to a basal spacing of ~3.8 and 1.3 nm, respectively. Previous work [13] has shown a peak for Na hectorite powder around $2\theta = 6°$ (1.5 nm); the peak we observe at 6.9° for Li hectorite is attributed to the corresponding clay platelet spacing that is contracted due to the smaller Li cations. The Na hectorite used by Cool and Vansant [13] had a platelet diameter of 2000 nm and was found naturally, whereas we used a synthetic Li-hectorite of 250 nm diameter, which could account for small differences between the two. The low angle peak at 2.3°, which is significantly broadened toward higher angle, has not previously been described. This feature is not a result of our sample processing as it is also observed in the as received sample of Na-Hectorite. It is conceivable that the low-angle peak at 2.3° is indicative of super lattice structures resulting from different size stacks of clay platelets. We have ensured that no divalent or stray metal ions are in the clay through elemental analysis (Table 1). The carbon content of around 0.1%, suggests that organic cations may be present from the manufacturing process, which would affect the spacing. Furthermore, the presence of the peak at 2.3° in Na hectorite diffractograms confirms that methanol used in the exchange process did not cause the increase in layer spacing.

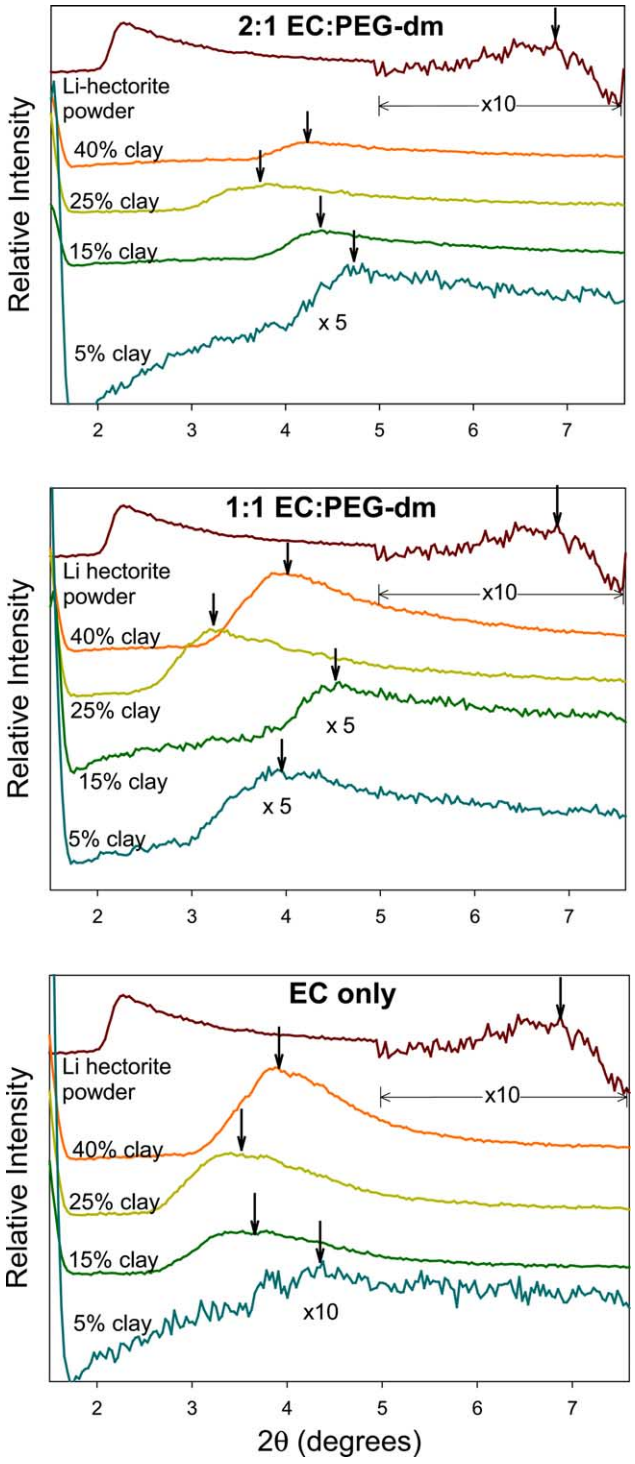

Fig. 4. XRD results for 2:1 EC:PEG-dm, 1:1 EC:PEG-dm, and EC only with 5, 15, 25, and 40% clay. Arrows indicate the peaks used to calculate the basal spacings plotted in this figure. The powder spectrum for Li hectorite is also shown.

The XRD peaks of the composite electrolytes are indicated by arrows on Fig. 4 and fall between $2\theta = 3.4$–4.7°. These peaks represent a low angle shift of the 6.9° peak seen in the Li hectorite diffraction pattern consistent with clay platelet swelling, i.e., an increase in platelet basal spacing (d_{001}). When plotted as a function of clay concentration (Fig. 5) it is evident that the clay swelling reaches a maximum 23–25 Å at about 25% clay loading.

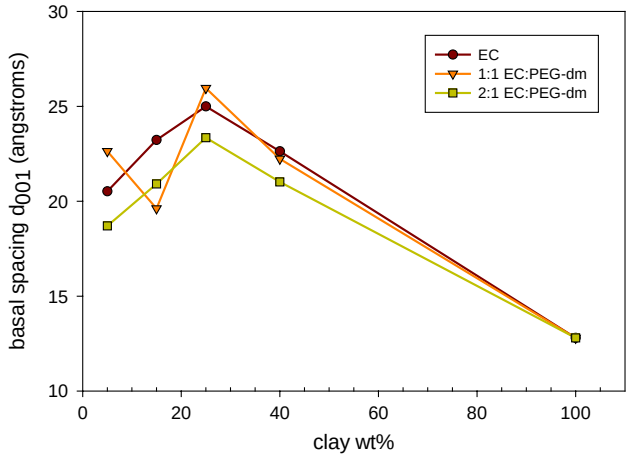

Fig. 5. Basal spacing for various Li-hectorite concentrations in 1:1 EC:PEG-dm, 2:1 EC:PEG-dm and EC only solvents.

3.3. Rheology measurements

Fig. 6 shows a representative plot of the elastic (G') and viscous (G'') moduli as functions of frequency for a 1:1 EC:PEG-dm solvent mixture at 5 and 15% clay content. Both G' and G'' are independent of frequency with G' exceeding G''. These features, which are characteristics of a gel [14], were found for all samples used in this study. Fig. 6 also shows that G' and G'' increase with clay concentration. The effect of clay concentration is clearly demonstrated in Fig. 7, which shows G' as a function of clay concentration for 1:1 EC:PEG-dm, 2:1 EC:PEG-dm, and 1:1 EC: PEG electrolytes at one frequency ($\omega = 1$ rad/s). Both gels with

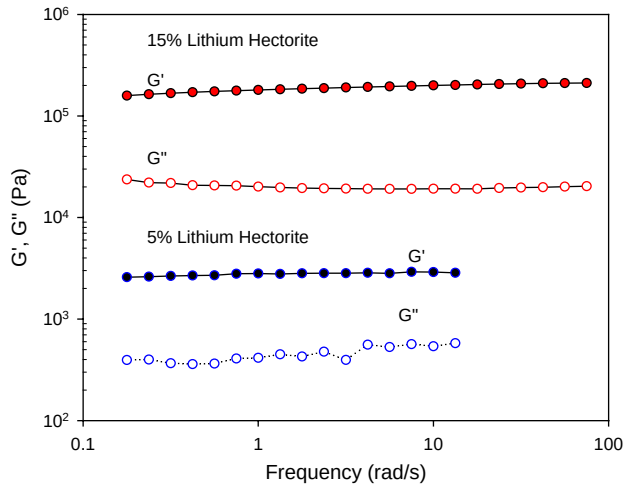

Fig. 6. G' (elastic modulus) and G'' (viscous modulus) as a function of frequency (at constant stress in the LVE regime) for 5 and 15% clay in 1:1 EC:PEG-dm.

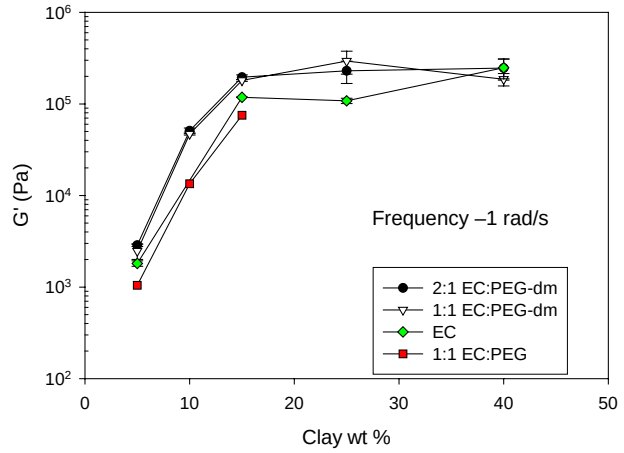

Fig. 7. Elastic modulus (G') at different Li-hectorite concentrations for four solvents: 1:1 EC:PEG-dm, 2:1 EC:PEG-dm, EC, and 1:1 EC:PEG.

PEG-dm present in the solvent display similar modulus in the concentration regime measured; however, the PEG gels exhibit lower G' values. Gel modulus for all samples increase by almost two orders of magnitude over the concentration range studied (5–40%).

Apparent yield stress was determined from a plot of G' as a function of stress amplitude [15,16]. Fig. 8 shows an example of this procedure for three samples: 10% clay in 1:1 EC:PEG, 5% in 1:1 EC:PEG-dm, and 10% in 1:1 EC:PEG-dm. Above a certain stress, the sample microstructure is disrupted with a concomitant decrease in G' and increase in G'' (G'' not shown in figure). The yield stress corresponds to the intersection of extrapolated lines drawn through the stress-invariant and stress-varying regimes, as shown by the arrows. Yield stress obtained using this approach for various samples at different concentrations of clay are provided in Table 2. Consistent with the trend in elastic modulus, the yield stress increases with clay concentration and the PEG-containing samples show lower yield stress when compared to PEG-dm-containing samples of the same clay concentration.

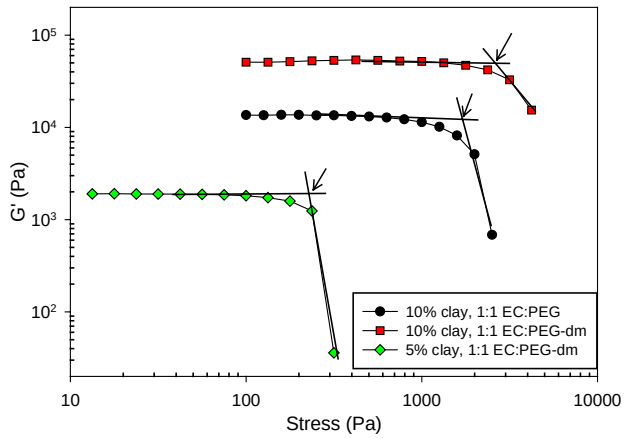

Fig. 8. Yield stress (marked by arrow) of 10 and 5% clay in 1:1 EC:PEG-dm and 10% clay in 1:1 EC: PEG.

Table 2
Yield stress (Pa) for 1:1 EC:PEG and 1:1 EC:PEG-dm electrolytes at various clay wt.%

Hectorite (%)	1:1 EC:PEG	1:1 EC:PEG-dm
5	160	230
10	1600	3000
15	4000	6000
20	5000	N/A

Table 3
Steady state creep compliance, J_e^o (Pa^{-1}), for 1:1 EC:PEG-dm and 1:1 EC:PEO solvent systems at various wt.% of Li-hectorite

Hectorite (%)	1:1 EC:PEG-dm	1:1 EC:PEO
10	3.7×10^{-5}	1.0×10^{-4}
15	1.3×10^{-5}	2.6×10^{-5}
20	N/A	1.3×10^{-5}

The steady state creep compliances J_e^o of samples are tabulated in Table 3. The creep compliance decreases with increasing clay concentration, and the PEG samples reveal a higher creep compliance compared to their methyl-capped analog. These results indicate that samples with larger clay content deform (or "creep") less under an applied stress.

The recoverable creep compliances (J_r) of Li hectorite samples in 1:1 EC:PEG-dm and 1:1 EC:PEG solvents at different clay concentrations are shown on a plot of strain normalized with respect to imposed stress (γ/τ_0) as a function of time (Fig. 9). While clay concentrations have a large effect on recovery, it is interesting to note that the strain recovery is larger for samples with lower clay concentrations.

4. Discussion

4.1. Effects of hectorite concentration

Ionic conductivity is dependent on both concentration and mobility of the ions. The later is affected by electrolyte viscosity and, in the Li-hectorite composite system, filler dispersion. Increase in viscosity and clay platelet aggregation can impede mobility and lower conductivity. Ion concentration is proportional to clay content, yet the higher the clay concentration, the more likely is platelet aggregation. This proportionality leads to a maximum conductivity at an optimum clay concentration, which has also been shown previously by Riley et al. [10] for carbonate solvents. We find broad maxima in conductivity as a function of clay concentration for the PEG-dm-containing electrolytes (Fig. 2). We also note a correlation between conductivity and platelet separation maximum with respect to clay concentration.

Clay platelets have been shown by Krishnamoorti et al. [17] and Luckham and Rossi [18] to experience self interactions which affect their geometrical arrangement. In these single-ion conductors, the self-interactions affect conductivity because the platelets create channels for ion

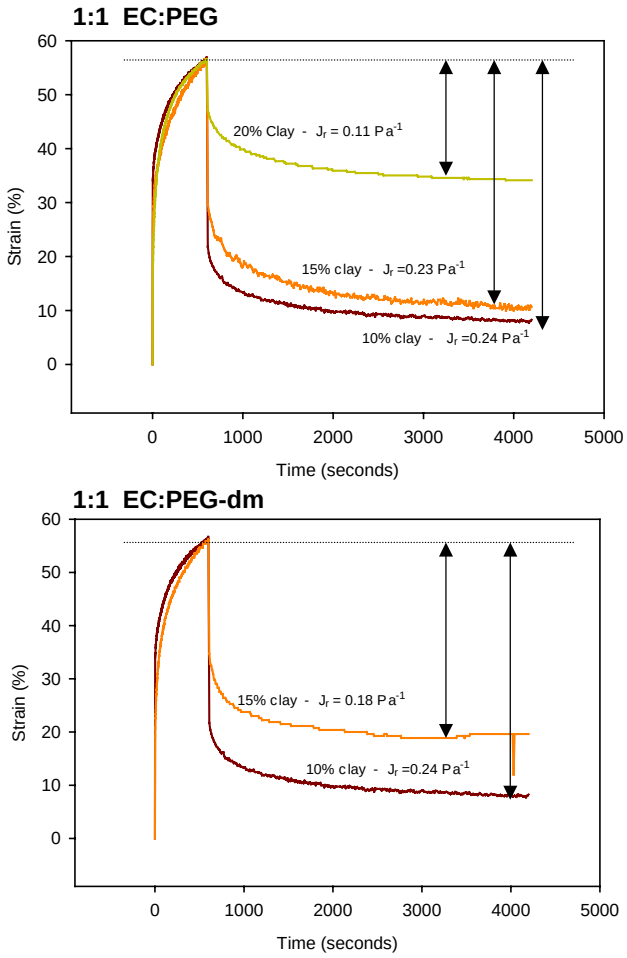

Fig. 9. Creep measurements for 1:1 EC:PEG and 1:1 EC:PEG-dm at various loadings of Li-hectorite. Curves are normalized to show comparative relaxation. The vertical arrows represent the recoverable creep compliance J_r for each sample.

movement. Various modes of platelet associations (dispersed, face-to-face, edge-to-face, and edge-to-edge), alter the channels for lithium-ion movement and hence conductivity. Clay platelets are stable in suspensions because of electrical double-layer repulsion. However, at high concentration of clay, interlayer repulsion decreases and platelets aggregate. When platelets aggregate, conductivity decreases because lithium-ions are less mobile between platelets. We found that ~25% clay yields the best balance of Li^+ concentration (0.22 mol Li^+/kg solvent) and clay platelet separation.

The average separation of platelets is significantly influenced by its concentration in the polymer solvent, as verified by XRD measurements (Fig. 5). At 25% clay concentration, the basal spacing reaches a maximum for all solvents studied (23–26 Å) and declines as clay concentration increases (Fig. 5). The conductivity follows the same trend with a maximum at 25% clay composition. However, the decrease in conductivity at higher concentration of clay (Fig. 3) is less pronounced than the contraction of the basal spacing because of the beneficial effect on conductivity of increased charge-carrier concentration with more clay. The basal spacing and conductivity results indicate that platelets are separated best for single-ion mobility at a concentration of 25% clay (in both 2:1 EC:PEG-dm and EC solvents).

At high concentrations of clay the double-layer collapse leads to closer platelets, while at low concentrations (5 and 15% clay) the platelets are more randomly oriented, which are unlike the ordered face-to-face, edge-to-edge, or edge-to-face structures and appear as a broad XRD peak of low intensity [13]. A broad peak represents a wide distribution of particle spacing, typical of platelets that are near exfoliation (5 and 15% clay samples). TEM images [19,20] show a stacking effect of clay layers when embedded in resin. These stacks of clay layers, ranging from 2 to 4 in number, constitute one clay particle. High intensity XRD peaks, as seen at 25 and 40% clay concentrations, represent stacks of clay platelets with uniform spacing between the particles ($3.0 < 2\theta < 4.5^\circ$). A schematic of platelet stacks and interplatelet spacing is shown in Fig. 10. The progression from more clay particles (Fig. 10a) to less clay particles (Fig. 10d) corresponds to a decrease in uniformity of basal spacing.

4.2. Polymer concentration effect

One objective of this research was to observe the change in conductivity upon addition of low-molecular weight polymer to a nanocomposite clay-based electrolyte. We found that a EC:PEG-dm (250 MW) solvent mixture, at a 2:1 volumetric ratio, produced electrolytes with the highest conductivity (Figs. 2 and 3). At higher content of PEG-dm, such as 1:1 EC:PEG-dm, conductivity decreased slightly and was similar to the EC only samples. These results indicate PEG-dm addition can be beneficial to ionic conductivity when a small amount is added to the carbonate co-solvent. The dielectric constants for EC and PC [21], $\varepsilon = 89$ and 64, respectively, are greater than that of PEG-dm 250 MW ($\varepsilon = 7.9$) [21], hence PEG-dm alone is not as conducive to salt disassociation as EC or PC. Surprisingly, the conductivity of 1:1 EC:PEG-dm and 1:1 EC:PC electrolytes are similar despite the higher dielectric constant of the 1:1 EC:PC mixture. We believe that gel formation, and thus the conductivity, in the samples is controlled more by the concentration of clay platelets than the solvent type. This is consistent with the rheology results, as discussed later. However, because of the a slight increase in conductivity when small amounts of PEG-dm are added to EC (2:1 EC:PEG-dm), we expect that interactions (Van der walls, dipole/dipole, etc.) between PEG-dm molecules and clay platelets exist to affect electrolyte structure.

4.3. Rheological properties of Li hectorite electrolytes

The rheological results indicate that clay concentration is a dominant factor in dictating the modulus/strength of

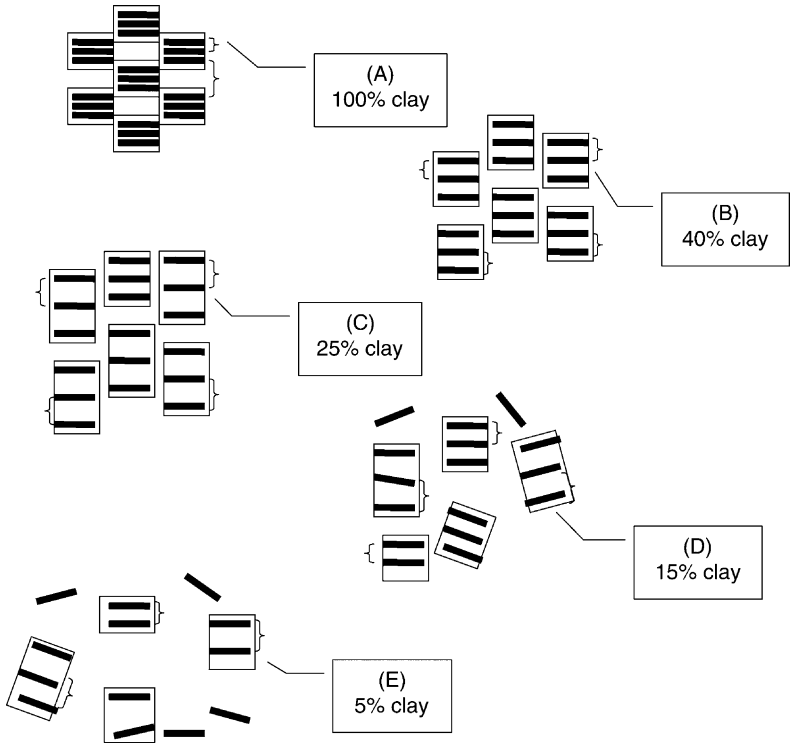

Fig. 10. Schematic of clay platelet aggregation. The horizontal bars represent clay platelets. The boxes around platelets represent collection of platelets that act as a group. Brackets signify examples of spacing detected by XRD. As the clay percentage decreases, (A) 100 (B) 40, (C) 25, (D) 15, and (E) 5%, and exfoliation increases, the variety of spacing become more apparent, leading to a broader XRD peak (Fig. 4).

the electrolytes. An increase of G' by almost two orders of magnitude ($\sim 10^3$ to $\sim 10^5$ Pa) was observed as clay weight percent increased from 5 to 15% (Fig. 7). At concentrations above 15% clay, the elastic modulus reaches a plateau, which represents declining change in inter-particle interactions. The nature or composition of the solvent seems to have a much smaller effect on modulus. For instance, G' is the same for 1:1 EC:PEG-dm and 2:1 EC:PEG-dm electrolytes. EC only electrolytes had slightly lower G' in comparison to PEG-dm-containing samples except at 40% loading, at which all sample have essentially identical G'. These results indicate that the platelet aggregates are influenced more by platelet/platelet interactions than solvent/clay interactions. The modulus of the EC:PEG samples decreases by only a factor 2–3 from the EC:PEG-dm samples, a difference that is small in comparison to the two orders of magnitude difference observed with changes in clay concentration. Because of strong electrostatic interactions between platelets, the small change in viscosity induced by doubling the PEG-dm:EC ratio from 1:1 to 2:1, does not affect the overall elastic modulus. In gels using PC:EC solvent studied by Riley et al. [22], the elastic moduli also fall in the range of values presented in the present study. Future investigations with higher molecular weight PEG-dm is of interest since it may show a greater effect on gel strength because of increase in polymer viscosity.

The lower elastic modulus observed for the EC:PEG electrolytes compared to EC:PEG-dm electrolytes (Fig. 7) can be explained in terms of the dispersion of clay in the solvent. Low-molecular weight hydroxyl terminated PEG is more polar than PEG-dm and will produce a better solvent/clay dispersion. In fact, electrolytes with 1:1 EC:PEG solvent were more translucent (i.e., better dispersed) than the PEG-dm mixtures. Because of the relatively more polar nature of the polymer, PEG exfoliates the clay layers, whereas PEG-dm does not solvate the platelets leading to clay aggregation. Such a scenario is consistent with the results of Riley et al. [22], who found that G' and yield stress decrease with enhanced dispersibility. In the present study, the yield stress of Li hectorite in 1:1 EC:PEG-dm is also consistently higher when compared to Li hectorite in 1:1 EC: PEG. Our results show that materials with high G' also have a high yield stress. While these are desirable rheological characteristics for an electrolyte, it is important for an electrolyte to exhibit minimum creep compliance. The steady state creep compliance, J_e^o, shown in Table 3, represents the deformation extent of an electrolyte and we find it to decrease with increasing clay concentration. This result is consistent with the modulus data, as we would expect a stronger gel to deform less than a weaker gel when the same stress is applied.

Interestingly, though the opposite trend is noticed in the material recovery, as quantified by the recoverable creep compliance (J_r). The J_r, which reflects the ductile/flexible

nature of the sample, increases with decreasing clay concentration. This result indicates that the electrolytes become less elastic with increasing clay concentration. We can rationalize this occurrence by realizing that, at high concentrations of clay the matrix of platelets is complex and once altered by stress, the matrix does not recover its original structure. The loss tangent data ($\tan\delta \equiv G''/G'$) from our dynamic experiments is also consistent with the recovery results. For instance, the loss tangents for samples containing 10, 15, and 20% clay in 1:1 EC:PEO, are 0.06, 0.08, and 0.09, respectively, and in 10 and 15% clay with 1:1 EC:PEG-dm solvent tan δ is 0.06 and 0.10, respectively. This indicates that while addition of clay increases elastic modulus it has a larger effect in enhancing viscous modulus. The relative increase in viscous contribution also manifests itself in the samples by becoming less elastic or ductile with higher clay concentrations.

5. Conclusions

We examined the effects of Li hectorite clay concentration and solvent composition on the conductivity and rheology of nanocomposite single-ion conductors. All samples exhibit gel-like behavior with room temperature conductivities of order 0.1 mS/cm. A maximum in conductivity is observed with clay concentration of about 25%. A maximum in clay basal spacing is also observed in the same concentration range, suggesting a direct correlation between conductivity and basal spacing. In contrast, the elastic modulus increases with clay concentration and asymptotes to 2×10^5 Pa at about 15% clay. These results taken together indicate that while changes in basal spacing are important to conductivity, the rheology is not significantly affected by changes at such a small scale. Solvent composition seems to play a secondary role in terms of affecting both conductivity and rheology. Addition of PEG-dm to the base EC electrolyte produces moderate improvement in conductivity; the elastic modulus also increases by a factor of three. On the contrary, changes in clay concentration over a span of 5–15 wt.%, enhances G' and yield stress by two orders of magnitude and conductivity by one order of magnitude, clearly indicating clay concentration to be a key factor in determining the characteristics of these single-ion conductors.

Acknowledgements

This research was supported by the Department of Education, Graduate Assistance in Areas of National Need (GAANN) Electronic Materials Fellowship.

References

[1] R.J. Brodd, Recent developments in batteries for portable consumer electronics applications, Interface 8 (1999) 20–23.
[2] L. Xie, D. Fouchard, S. Megahed, Material requirements for lithium-ion batteries, in: Proceedings of the Material Research Society Symposium, vol. 393, San Francisco, CA, 1995, pp. 285–304.
[3] A. Tether, Scientist Helping America, http://safe.sysplan.com/scihelpamerica/ad.html, 2002.
[4] L. Gaines, R. Cuenca, Costs of Lithium-ion Batteries for Vehicles, 2000.
[5] M. Wakihara, Recent developments in lithium ion batteries, Mater. Sci. Eng. R-Rep. 33 (2001) 109–134.
[6] S.R. Raghavan, M.W. Riley, P.S. Fedkiw, S.A. Khan, Composite polymer electrolytes based on poly(ethylene glycol) and hydrophobic fumed silica: dynamic rheology and microstructure, Chem. Mater. 10 (1998) 244–251.
[7] Y.X. Li, P.S. Fedkiw, S.A. Khan, Lithium/V6O13 cells using silica nanoparticle-based composite electrolyte, Electrochim. Acta 47 (2002) 3853–3861.
[8] J. Fan, S.R. Raghavan, X.Y. Yu, S.A. Khan, P.S. Fedkiw, J. Hou, G.L. Baker, Composite polymer electrolytes using surface-modified fumed silicas: conductivity and rheology, Solid State Ionics 111 (1998) 117–123.
[9] H.J. Walls, J. Zhou, J.A. Yerian, P.S. Fedkiw, S.A. Khan, M.K. Stowe, G.L. Baker, Fumed silica-based composite polymer electrolytes: synthesis, rheology, and electrochemistry, J. Power Sources 89 (2000) 156–162.
[10] M. Riley, P. Fedkiw, S. Khan, Transport properties of lithium hectorite-based composite electrolytes, J. Electrochem. Soc. 149 (2002) A667.
[11] P. Aranda, E. Ruiz-Hitzky, Poly(ethylene oxide)/NH^{4+}-smectite nanocomposites, Appl. Clay Sci. 15 (1999) 119–135.
[12] S.A. Khan, C.A. Schnepper, R.C. Armstrong, Foam Rheology. III. Measurements of shear flow properties, J. Rheol. 32 (1988) 69–92.
[13] P. Cool, E.F. Vansant, Preparation and characterization of zirconium pillared laponite and hectorite, Microporous Mater. 6 (1996) 27–36.
[14] C.W. Macosko, Rheology: Principles, Measurements, and Applications, VCH, New York, 1994.
[15] H.J. Walls, B.S. Cains, A.M. Sanchez, S.A. Khan, Yield stress and wall slip phenomena in colloidal silica gels, J. Rheol. 47 (2003) 847–868.
[16] M.C. Yang, L.E. Scriven, C.W. Macosko, Some rheological measurements on magnetic iron-oxide suspensions in silicone oil, J. Rheol. 30 (1986) 1015–1029.
[17] R. Krishnamoorti, J. Ren, A.S. Silva, Shear response of layered silicate nanocompostites, J. Chem. Phys. 114 (2000) 4968–4973.
[18] P.F. Luckham, S. Rossi, The colloidal and rheological properties of bentonite suspensions, Adv. Colloid Interf. Sci. 82 (1999) 43–92.
[19] J.F. Alcover, Y. Qi, M. Al-Mukhtar, S. Bonnamy, F. Bergaya, Hydromechanical effects: (I) on the Na-smectite microtexture, Clay Miner. 35 (2000) 525–536.
[20] H.J. Walls, M.W. Riley, R.R. Singhal, R.J. Spontak, P.S. Fedkiw, S.A. Khan, Nanocomposite electrolytes derived from fumed silica and hectorites: passive versus active fillers, Adv. Funct. Mater. 13 (2003) 710–717.
[21] S.R. Raghavan, H.J. Walls, S.A. Khan, Rheology of silica dispersions in organic liquids: new evidence for solvation forces dictated by hydrogen bonding, Langmuir 16 (2000) 7920–7930.
[22] M. Riley, P. Fedkiw, S.A. Khan, Nanocomposite based electrolytes for lithium-ion batteries, Mater. Res. Soc. Symp. Proc. 575 (2000) 137–142.